



Planetary Systems Demographics: The View from High-Resolution Spectroscopy

A. Sozzetti¹

Istituto Nazionale di Astrofisica – Osservatorio Astrofisico di Torino, Via Osservatorio 20, I-10025 Pino Torinese, Italy e-mail: alessandro.sozzetti@inaf.it

Received: 06-12-2022; Accepted: 07-02-2022

Abstract. I present a brief overview of the demographics of exoplanetary systems at short and intermediate orbital separations. The primary focus of this review is on the results obtained with (ultra-)stable, high-resolution spectrographs capable of delivering (very) high-precision radial velocities. The key contributions of high-resolution spectroscopy (HRS) to the characterization of exoplanetary atmospheres is also addressed. I highlight in particular the present and expected contributions to the field made by ongoing (e.g., HARPS-N/TNG, ESPRESSO/VLT) and future (e.g., ANDES/ELT) programs in which the Italian community plays key roles.

Key words. Planetary systems – Planets and satellites: detection – Planets and satellites: composition – Techniques: radial velocities – Techniques: spectroscopic – Methods: data analysis – Methods: numerical

1. Introduction

High-resolution stellar spectroscopy has long been recognized as a powerful tool for the detection of extrasolar planets. Struve (1952), in presenting the determination of the frequency of planet-like bodies orbiting stars other than the Sun as one of Astronomy's burning questions, was already suggesting that the measurement of time-series of stellar radial velocities (RVs) would enable the detection of such companions. Struve (1952) argued that discovering Jupiter-mass companions at Jupiter-like distances would be very much out of question, as they would induce RV variations of too small amplitude. However, he claimed there is no compelling reason not to expect them to be found at much closer distances. If orbiting with a 1-day period, they would cause RV os-

cillations with semi-amplitude $K \sim 200 \text{ m s}^{-1}$, which would be just about detectable with the most powerful spectrographs of the time.

Forty three years later, a stable RV signal with $K = 56 \text{ m s}^{-1}$ and a period of 4.23 days was detected by Mayor & Queloz (1995) based on a collection of 142 high-resolution stellar spectra of the nearby solar-type star 51 Pegasi gathered with the fiber-fed echelle spectrograph ELODIE mounted on the 1.93-m telescope of the Haute-Provence Observatory, delivering a typical RV precision of $\sim 10 \text{ m s}^{-1}$. With a mass of $0.47 M_{\text{Jup}}$, 51 Peg b was the first extrasolar planet detected around a normal star, and its discovery became Physics Nobel Prize worthy in 2019.

Today, the sample of discovered planets exceeds 5 000. As one can see in Fig. 1, Doppler

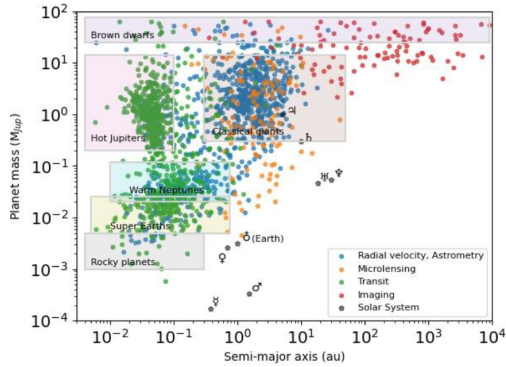


Fig. 1. Mass vs. orbital separation for the sample of known exoplanets and brown dwarfs. Color-coding highlights objects detected by different techniques. Approximate regimes of different planet classes are also shown. Data from <http://exoplanet.eu>.

measurements have contributed greatly to populating the mass-orbital separation parameter space, both alone and as key tool for the confirmation of the planetary nature of transit candidates. Since the discovery of 51 Peg b, RV precision has improved by over one order of magnitude, first achieving the 1 m s^{-1} level at the turn of the Century, and just recently attaining the few tens of cm s^{-1} level. The sensitivity of the RV technique is maximized at short and intermediate separations ($\leq 5 \text{ AU}$ or so), due to the combination of intrinsic precision and time baseline of the observations. It is in this regime that Doppler data have provided the most relevant contribution to our present understanding of the statistical properties of planetary systems across a very broad range of masses, reaching now even below 1 Earth mass. We have now entered the era of exoplanet demographics.

2. What is exoplanet demographics?

Studies of exoplanet demographics focus on determining the occurrence rate of planets as a function of as many of the physical parameters p_1, \dots, p_n that may influence planet formation and evolution as possible, over as broad of a range of these parameters as possible, and establish the existence of trends and correlations between them, or lack thereof. The parameters

include, but are not limited to, planetary properties (e.g., mass, radius, density, orbital separation, eccentricity, inclination, multiplicity) as well as host star characteristics (e.g., mass, age, chemical composition, binarity, birth environment).

The key quantity to determine is the:

$$\text{Occurrence Rate} = \frac{N_{pl}}{N_{\star}}, \quad (1)$$

where N_{pl} is the number of detected planets in a survey that have the stipulated properties and N_{\star} is the number of stars in a survey for which such planets could have been detected. Occurrence rates are typically calculated integrating over given intervals of the parameters the occurrence rate density:

$$\frac{d^n N_{pl}}{dp_1 \dots dp_n} = A f(p_1) \dots f(p_n), \quad (2)$$

Measuring the distribution functions of the relevant parameters is the ultimate goal of exoplanet demographics, as they retain the imprints of all the processes at work during planet formation and evolution. This is, however, not a trivial task, as an accurate measurement of occurrence rates requires a large sample of stars that have been searched for planets and the proper understanding of observational biases/selection effects that favor the discovery of certain types of planets. Robustly accounting for completeness (number of missed planets) and reliability (number of false positives) is a rather complex problem. I turn next to summarize some of the most relevant results in the field of close-in ($a \leq 5 \text{ AU}$ or so) exoplanet demographics achieved via RV measurements at high spectral resolution ($R > 50\,000$). Where appropriate, I will emphasize the particular contributions made by Guaranteed Time Observations (GTO) programs and other large programs such as the Italy-led Global Architecture of Planetary Systems (GAPS) that have exploited large RV datasets gathered with the very high-resolution ($R > 100\,000$), ultra-stable, visible spectrographs HARPS-N (Cosentino et al. 2012) and ESPRESSO (Pepe et al. 2021), which routinely deliver state-of-the-art RV

with $\sim 1 \text{ m s}^{-1}$ and $\sim 10 \text{ cm s}^{-1}$ precision, respectively.

3. Demographics of close-in planets

3.1. Distribution functions

Both long-term Doppler surveys and spaceborne transit programs, in particular the Kepler mission (Borucki et al. 2010) have provided spectacular observational data that have allowed to determine the distribution functions of orbital and physical parameters of close-in exoplanets. For example, since a decade now we know that the mass and radius distributions are steep increasing functions of decreasing mass and radius (e.g., Howard 2013). Planets with the size and mass not very different from those of the Earth (the so-called super-Earths) are at least one order of magnitude more common than gas giants: about 30% of solar-type stars hosts one such planet. At intermediate separations, high-precision, decades-long RV surveys have confirmed the trend of increasing frequency of giant planets with increasing orbital period, up to $\sim 5 \text{ yr}$ ($\sim 3 \text{ au}$). This roughly corresponds to the location of the snow line in protoplanetary disks around solar-type stars (e.g., Mulders et al. 2015; Morbidelli et al. 2016). Beyond 3 au or so, the agreement of Doppler surveys appears to degrade sharply with orbital separation. Some studies indicate the presence of a decline in giant planet occurrence with increasing separation (Fernandes et al. 2019; Fulton et al. 2021), others (Wittenmyer et al. 2020) find no evidence of a turnover in giant planet frequency at the snowline. The distribution of orbital eccentricities of Doppler-detected planets encompasses the full range of possible values up to $e \sim 1.0$, it strongly correlates with orbital separation (very short-period planets lying on tidally circularized orbits), and it can be approximated by a Beta distribution (Kipping 2013). For an in-depth review of distribution functions of exoplanet parameters, see e.g. Biazzo et al. (2022).

3.2. The star-planet connection

The results from RV surveys have allowed to explore the dependence of planet occurrence on stellar properties. In particular, giant planet frequency increases sharply with increasing stellar metallicity for F-G-K dwarfs (Fischer & Valenti 2005; Sozzetti et al. 2009; Mortier et al. 2012; Adibekyan 2019), while whether small-planet occurrence correlates positively with metallicity in the same stellar samples is still a matter of debate (Adibekyan 2019; Sousa et al. 2019; Bashi et al. 2020). Hot-Jupiter occurrence rates around stars more massive than the Sun appear lower than those determined around Solar-type primaries (Sebastian et al. 2022). The occurrence rate for giant planets within 3 au increases with host star mass up to $\sim 2 M_{\odot}$ (Johnson et al. 2010; Ghezzi et al. 2018; Wolthoff et al. 2022), with low-mass M dwarfs hosting as few as 10 times less Jovian mass companions than solar-type stars (e.g., Endl et al. 2006; Bonfils et al. 2013; Tuomi et al. 2014). At the high host-star mass end, giant planet occurrence rates are based on RV monitoring of giant stars, with possible uncertainties due to false positives of stellar origin, particularly oscillatory convective modes (Wolthoff et al. 2022, and references therein). On the contrary, the occurrence rate of close-in super Earths around M dwarfs could be higher than that for F-G-K stars by a factor of 2-3 (Bonfils et al. 2013; Sabotta et al. 2021), it rises sharply with increasing orbital period (Pinamonti et al. 2022), and it presents weak or no correlation with mass and metallicity, respectively (Maldonado et al. 2020). Occurrence rates of small-mass planets from RV surveys are also potentially affected by false detections of stellar origin, typically stemming from activity signals in connection with the stellar rotation period (see e.g., Holl et al. 2022 for a summary of well-known systems containing Super-Earth-type companions of more or less dubious origin). Occurrence rate calculations based on Kepler mission data have reaffirmed the same trends and correlations with stellar parameters as outlined above (e.g., Petigura et al. 2018; Hsu et al. 2019; Kunimoto & Matthews 2020; Yang et al. 2020;

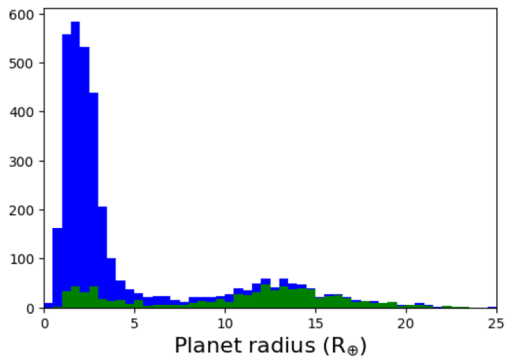


Fig. 2. Blue histogram: Radius distribution of transiting exoplanets. The green histogram indicates the sub-sample of planets with dynamical mass, and therefore density, determination. Figure credits: A. Mortier.

Beleznyay & Kunimoto 2022). False positives are a concern for transit surveys as well. A classical example is provided by the apparent discrepancy of a factor ~ 2 in hot-Jupiter frequency around solar-type stars as measured by the Kepler (Howard et al. 2012; Fressin et al. 2013) and CoRoT (Deleuil et al. 2018) missions, respectively, which was only recently reconciled (Wang et al. 2021; Beleznyay & Kunimoto 2022).

3.3. The mass-radius diagram

The mass-radius diagram for transiting exoplanets is the fundamental tool that allows to directly compare the observational data with structural models, expressed in terms of iso-density curves that describe the mass-radius relation for a fixed composition (e.g., Zeng et al. 2019). Precise masses/densities of planets are also key to estimate their atmospheric scale heights and thus select those best suited for atmospheric characterization, both from the ground (with e.g., HARPS, HARPS-N, ESPRESSO, GIANO-B, Spirou, NIRPS, etc.) and in space (with e.g. HST, JWST and Ariel). Precise densities and therefore well-constrained compositions are particularly important for small planets (Batalha et al. 2019). However, this is a difficult task: as we see in Figure 2, the vast majority of small-radius

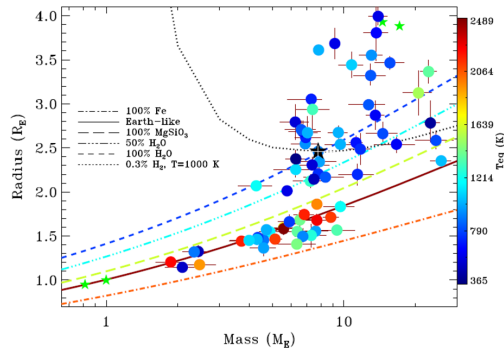


Fig. 3. Mass-radius diagram for small ($R < 4 R_{\oplus}$) transiting exoplanets with an RV-based dynamical mass determination at the 3σ level or better. Objects are color-coded according to their T_{eq} . The different curves depict internal structure models of a variable composition from Zeng et al. (2019) (as reported in the legend). Green stars show the locations of Solar-System planets. Data from the TEPcat catalog (<https://www.astro.keele.ac.uk/jkt/tepcat/>) as of September 2021.

planets ($R \leq 4 R_{\oplus}$, below the radius of Neptune) does not yet have a dynamical mass measurement through Doppler spectroscopy.

As shown in Figure 3, the mass-radius diagram of small planets with well-determined masses (better than 30% precision) allows today to identify two broad classes of planets, super-Earths with primarily rocky, and often Earth-like, composition, and volatile-rich sub-Neptunes. The equilibrium temperatures T_{eq} of the former sample are typically higher than those of the latter sample. We tentatively see a lack of planets with radii of $\sim 1.8 R_{\oplus}$. The effect is due to the clear bimodality of the radius distribution, which shows a deficit of factor ~ 2 in occurrence (the radius valley or gap) in the range $1.5 - 2.0 R_{\oplus}$ (Fulton et al. 2017; Fulton & Petigura 2018). This prominent feature is understood today as primarily due to photoevaporation processes (e.g., Owen & Wu 2017). In the density vs. period diagram of Figure 4 we clearly notice the lack of very close-in low-density sub-Neptunes, which have lost their outer envelopes due to the strong irradiation from their parent stars. The apparent paucity of rocky planets on longer pe-

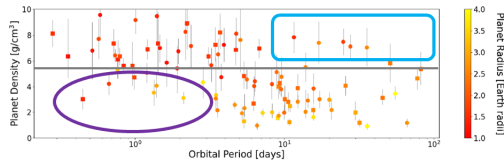


Fig. 4. Density as a function of orbital period for super Earths and sub-Neptunes. Objects are color-coded according to their radius. The blue and purple regions highlight the lack of low-density sub-Neptunes at very short periods and the paucity of rocky super-Earths on longer periods. Figure credits: *A. Mortier*.

riods is due to the present lack of sensitivity of the RV technique. In density space, small transiting planets around M dwarfs appear to more clearly belong to three distinct populations: rocky, water-rich, and gas-rich (Luque & Pallé 2022). It is particularly worth noticing how more than 50% of the systems shown in Figure 3 have their masses determined based on HARPS-N GTO RV measurements. This program has been extremely successful in measuring masses of small planets, including those with ultra-short periods (< 1 day), e.g., Malavolta et al. 2018; Cloutier et al. 2021), some with rather long periods (up to ~ 80 days, e.g., Mortier et al. 2018; Lacedelli et al. 2021), and most notably the first Earth-sized planet with an Earth-like density (Pepe et al. 2013).

3.4. Multi-planet systems

The average number of planets per star is a very difficult parameter to constrain precisely, because of the variety of selection effects and variable sensitivity to areas of the parameter space inherent to different detection techniques. A key question in the field of exoplanet demographics, for which we have yet to find the answer, is: 'Is the Solar System common?'. On the one hand, by comparison with the astonishing diversity of the orbital and physical properties of known planetary systems to-date, one would be inclined to draw the conclusion that the one we live in is unlike any other planetary systems, and the rate of occurrence of Solar-System analogs might be of the order of

a few percent, or lower (e.g., Schlaufman 2014; Mishra et al. 2023). On the other hand, the limited sensitivity of detection techniques to Solar-System-like architectures suggests that the fact that we have not yet found a true Solar System analog to-date is due, at least in part, to observational biases rather than an intrinsically low frequency of true analogs of the Solar System.

Planetary systems exhibit an extremely rich architectural diversity. The wealth of data from the Kepler mission has allowed to uncover ~ 1000 multiple transiting systems. They are found in very 'flat' configuration, with mutual inclination angles often well below 1 degree, and often in very compact, closely-spaced configurations of small-size ($R < 4 R_{\oplus}$) planets, with as many as five companions orbiting inside Mercury's orbit (e.g., He et al. 2019. See Biazzo et al. 2022 for a review summary). Most of the small planet pairs are not in exactly resonant configurations, but show excesses of near-resonant pairs (e.g., Choksi & Chiang 2020). Extensive studies of the population have revealed how multiplicity clearly correlates with both eccentricity and mutual inclination (e.g., He et al. 2020), size and spacing (e.g., Weiss et al. 2018).

The same patterns in the multi-planet system population have been uncovered by long-term Doppler surveys, albeit in the presence of lower number statistics (over 400 RV-detected multis are known to-date). Differences in e.g., the eccentricity distribution of singles and multis had already been highlighted by (Wright et al. 2009), with recent work highlighting the existence of the same correlation seen in Kepler data (e.g., Turrini et al. 2020). The high frequency of architectures in which an inner, small-mass companion is accompanied by a larger-mass outer planet (about 80% of the cases) observed in Kepler data (Ciardi et al. 2013) is also clearly measured in the RV sample. The structure of peaks and deficits near resonance in the period ratio distribution is also identified (see e.g., Biazzo et al. 2022). Compact systems of low-mass planets at short orbital separations, analogs of those found with small radii by the Kepler mission, are also unveiled by RV surveys, but their exact mul-

tiplicity is increasingly more difficult to determine with high statistical confidence due to their very low-amplitude RV signals (e.g., Udry et al. 2019).

High-resolution spectroscopic measurements with HARPS-N and ESPRESSO have critically contributed to the improved characterization of several multiple transiting systems. Notable examples include: a) density determination for six super-Earths and sub-Neptunes in a resonant chain with period ratios between 2:1 and 4:3 orbiting TOI-178 (Leleu et al. 2021); b) dynamical masses for two young, high-density gas giants orbiting the young solar-type star ν 1298 Tau, indicating that giant planets can contract much more quickly than usually assumed (Suárez Mascareño et al. 2021); c) density determination for two super-Earths with the same radius but very different masses in the Kepler-107 system, indicating that one of them (Kepler-107c) likely underwent a cataclysmic collision event early on (Bonomo et al. 2019); d) the determination of a large mutual inclination angle (< 50 deg) between a short-period transiting super-Earth and a long-period $13-M_{\text{Jup}}$ companion in the π Mensae system (Damasso et al. 2020).

3.5. The hunt for Earth-like planets

Figure 5 shows the fleet of space missions (NASA and ESA) and relevant ground-based instruments for HRS at medium, large telescopes and the ELT with a more or less primary focus on the detection and characterization of extrasolar planetary systems. They implement various elements of a detailed roadmap that has declined the ultimate goal of exoplanetary science in terms of the study of habitability conditions and the detection of atmospheric biosignatures of temperate terrestrial exoplanets that can be directly imaged around the nearest solar-type stars. The identification of the final achievement is driven by the need to address directly a fundamental question of Humankind: 'Are we alone'? Finding the targets first is mandatory in order to maximize the science return, and avoid spending precious observing time of ground-based instrumenta-

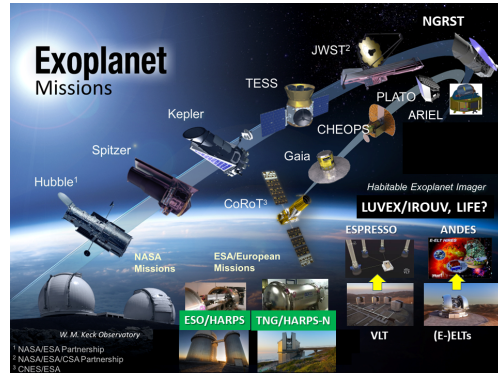


Fig. 5. Present and future exoplanet missions from space agencies and ground-based instruments at observatories around the world with a focus on high-resolution spectroscopy. Baseline figure credits: *NASA/JPL-Caltech*.

tion such as ELT/PCS (Kasper et al. 2021) or future space observatories such as NASA's LUVex/IROUV or the LIFE mission concept (Quanz et al. 2021) simply searching for such companions without prior knowledge of their existence. This is no easy task to accomplish. The technique more likely to attain such detections is expected to be the Doppler method, but we must keep in mind that the semi-amplitude of a 1-Earth minimum-mass companion at 1 au from a solar-mass star is only 9 cm s^{-1} , which is still below the single-measurement precision of ESPRESSO, and it is a signal very much likely buried underneath star-induced RV variations of at least one order of magnitude larger. A blind search for true Earth twins would benefit from prior knowledge on the likelihood of their occurrence.

The frequency of Earth-like planets, η_{\oplus} , is a much sought-after number. Most of the effort in estimating η_{\oplus} is based on results from the Kepler mission. Over the last decade, about 30 different estimates have been published, depending on a variety of assumptions such as range of planetary radii and range of primary mass. The most recent, sophisticated attempts, which correct for completeness and reliability, constrain the occurrence rate of Earth twins to lie in the approximate interval $\eta_{\oplus} \approx 5 - 50\%$ (see e.g., Bryson et al. (2021) for details). The value of η_{\oplus} is however still in practice an ex-

trapolation, as we do not have an actual piece of direct observational evidence yet.

The sample of temperate terrestrial planets (radius $< 1.5 R_{\oplus}$, minimum mass $< 3 M_{\oplus}$) amounts today to about 20. It is evenly split between objects detected by transit surveys and companions found with the Doppler method. They all orbit much cooler primaries than our Sun and, with one exception, we have no information on their actual density, as no mass determination has been achieved for those that transit, while those detected in Doppler programs do not transit, so there is no radius measurement available. The one exception is the TRAPPIST-1 system (Gillon et al. 2017), whose transiting temperate companions have mass estimates from the transit timing variation technique: the star is an ultra-cool M8 dwarf with just about 8% the mass of the Sun, and it's too faint for attempting dynamical mass measurements with RVs.

The temperate terrestrial minimum-mass planets found via high-resolution Doppler spectroscopy around some of the nearest low-mass M dwarfs include some very intriguing cases. The most notable example is the $m_p \sin i = 1.2 M_{\oplus}$ companion orbiting in the habitable zone of the nearest star to the Sun, Proxima Centauri ($M_{\star} = 0.12 M_{\odot}$), initially detected by Anglada-Escudé et al. (2016) and more recently confirmed based on ESPRESSO measurements (Suárez Mascareño et al. 2020). Always thanks to ESPRESSO GTO RV data, the Proxima system was very recently found to host another planet interior to Proxima b, inducing an RV signal of $\sim 40 \text{ cm s}^{-1}$ (corresponding to $m_p \sin i \sim 0.3 M_{\oplus}$), which is today the record-holder in terms of smallest RV amplitude ever detected (Faria et al. 2022). At the high-mass end of the primary, Damasso et al. (2022) recently uncovered the presence of a $m_p \sin i = 5.2 M_{\oplus}$ super-Earth with an orbital period $P = 140$ days on a highly eccentric orbit ($e = 0.45$) that makes it move in and out of the habitable zone of its $0.5 M_{\odot}$ primary. To-date, the habitable-zone super-Earth with a preliminary density estimate found around the star closest in mass to our Sun is K2-3 d, orbiting with $P \approx 45$ days its $0.6 M_{\odot}$ primary (Damasso et al. 2018). The push towards the

identification of temperate Earth-sized, Earth-mass objects around Sun-like stars continues, with high hopes to reach the goal for both transiting systems thanks to the PLATO mission (Rauer et al. 2014) and for companions that can be directly imaged around the nearest stars based on the operations of ultra-high-precision RV instruments, of which ESPRESSO is the first, extremely successful example.

4. Exoplanet atmospheres

The classes of close-in transiting planets and young, wide-separation directly imaged gas giants are amenable to detailed spectroscopic characterization studies of their atmospheres. The most scientifically valuable measurements of exoplanetary atmospheres are those rigorously constraining their composition (atomic and molecular abundances and their ratios), vertical temperature structure, dynamics (circulation) and possible presence of altitude-dependent cloud decks and hazes (e.g., Madhusudhan et al. 2014).

The bulk of the atmospheric characterization studies has been obtained via detection of planetary thermal emission and transmission spectra gathered at low spectral resolution. In space, HST low-resolution spectroscopy (LRS) observations until very recently provided the most spectacular transmission and emission spectroscopy results for transiting planets (e.g., Madhusudhan 2019 and references therein), while from the ground low-resolution spectra of directly-imaged giant planets have been gathered using high-contrast imagers such as SPHERE/VLT (Beuzit et al. 2019). The James Webb Space Telescope (JWST) has just begun revolutionizing the field with the first outstanding results from the Early Release Science programs, in particular the first-ever detection of sulfur dioxide in the atmosphere of the hot Jupiter WASP-39 b (Alderson et al. 2022). Towards the end of the decade, the Ariel mission (Tinetti et al. 2018) will further contribute to the understanding of the full demographic spectrum of exoplanet atmospheres based on the largest expected sample of analyzed systems (~ 1000).

HRS has recently emerged as a powerful, complementary approach to LRS for characterizing exoplanet atmospheres. It is capable of resolving molecular bands into individual lines and of detecting the planet's Doppler shift directly. Detection of the peculiar fingerprint of individual molecules is obtained through cross-correlation with model templates. Since the pioneering detection of carbon monoxide (CO) by Snellen et al. (2010), and until the first just-published JWST ERS results, HRS both in emission and transmission is the only technique to have reliably detected atomic and molecular species in the atmospheres of transiting and non-transiting close-in exoplanets. At visible wavelengths, a plethora of neutral and ionized atomic species in the atmospheres of hot and ultra-hot ($T_{\text{eq}} \geq 2000$ K) Jupiters has been detected, including Ba, Co, Sr, Fe, Mg, Mn, Ti, V, K, Li, Ca, Cr, Na, Ni, Sc, Si, as well molecular compounds such as TiO and VO. Key results have been obtained by HARPS-N and ESPRESSO for several of the systems (e.g., Ehrenreich et al. 2020; Allart et al. 2020; Tabernero et al. 2021; Pino et al. 2020; Borsa et al. 2019, 2021a,b, 2022; Azevedo Silva et al. 2022). Detections of atomic species have also been obtained with other important instruments, such as CARMENES and ESPaDOnS (e.g., Cont et al. 2022). In the near-infrared, planetary absorption from the He I triplet line at 1083.3 nm (a proxy for the presence of an extended or escaping atmosphere) has been successfully detected in the atmospheres of several hot Jupiters with GIANO (Guilluy et al. 2020) and CARMENES (e.g., Allart et al. 2018; Nortmann et al. 2018; Salz et al. 2018; Alonso-Floriano et al. 2019). Until recently only molecular detections of CO and H₂O had been reported at high spectral resolution in the near-infrared (e.g., Brogi et al. 2012, 2014, 2018; Birkby et al. 2017; Cabot et al. 2019). Exploiting the very wide, simultaneous wavelength coverage (0.9 – 2.45 μm) of the GIANO near-infrared spectrograph at the TNG, Guilluy et al. (2019) unveiled for the first time the presence of CH₄ in emission in the atmosphere a non-transiting hot Jupiter. HRS data with GIANO became key for the si-

multaneous detection of six molecules (H₂O, CH₄, HCN, NH₃, C₂H₂) in transmission in the atmosphere of the hot Jupiter HD 209458 b (Giacobbe et al. 2021). Very recently multiple (up to five) molecular species were also detected with high statistical significance in the atmospheres of the two warm Jupiters WASP-69 b (Guilluy et al. 2022a) and WASP-80 b (Carleo et al. 2022), demonstrating for the first time that this class of planets also presents a rich atmospheric chemistry.

The outlook on characterization measurements of exoplanet atmospheres is very bright. The effective combination of both LRS and HRS data, which is presently a developing field of activity (Brogi et al. 2017; Brogi & Line 2019; Guilluy et al. 2022b), will provide tight constraints on molecular abundances, atmospheric elemental ratios (e.g., the C/O, N/O, and C/N ratios) and metallicities. This in turn will allow for much improved understanding of the physical and chemical processes in exoplanetary atmospheres and interiors, eventually placing key constraints on planet formation and evolution. Future joint HRS+LRS analyses will benefit from the contributions from both existing (GIANO, CARMENES, CRIRES+) and new (Spirou, NIRPS) high-resolution instruments at 4m- and 8m-class telescopes. Further down the line, the visible and near-infrared (0.4 – 1.8 μm) spectrograph ANDES (formerly known as HIRES, see Marconi et al. 2021) on the ELT will break new ground in combination with JWST and Ariel, aiming in particular at transmission spectroscopy of the atmospheres of temperate terrestrial planets transiting low-mass M dwarfs.

Acknowledgements. I warmly thank the scientific organizing committee for giving me the opportunity to deliver the talk at the HACK-100 Conference out of which this manuscript was born. The most well-studied classes of stars by Margherita Hack, i.e. supergiants, cataclysmic variables, and symbiotic systems, are definitely not the targets of planet searches at high spectral resolution. I am however confident that, given her keen interest in the subject of the search for life in the Universe, Margherita would have been very interested to discuss the ongoing developments in the field of exoplanet demographics, 'normal' as the host stars may be.

References

- Adibekyan, V. 2019, *Geosciences*, 9, 105
- Alderson, L., Wakeford, H. R., Alam, M. K., et al. 2022, arXiv e-prints, arXiv:2211.10488
- Allart, R., Bourrier, V., Lovis, C., et al. 2018, *Science*, 362, 1384
- Allart, R., Pino, L., Lovis, C., et al. 2020, *A&A*, 644, A155
- Alonso-Floriano, F. J., Snellen, I. A. G., Czesla, S., et al. 2019, *A&A*, 629, A110
- Anglada-Escudé, G., Amado, P. J., Barnes, J., et al. 2016, *Nature*, 536, 437
- Azevedo Silva, T., Demangeon, O. D. S., Santos, N. C., et al. 2022, *A&A*, 666, L10
- Bashi, D., Zucker, S., Adibekyan, V., et al. 2020, *A&A*, 643, A106
- Batalha, N. E., Lewis, T., Fortney, J. J., et al. 2019, *ApJ*, 885, L25
- Beleznav, M. & Kunimoto, M. 2022, *MNRAS*, 516, 75
- Beuzit, J. L., Vigan, A., Mouillet, D., et al. 2019, *A&A*, 631, A155
- Biazzo, K., Bozza, V., Mancini, L., & Sozzetti, A. 2022, in *Astrophysics and Space Science Library*, Vol. 466, *Demographics of Exoplanetary Systems*, Lecture Notes of the 3rd Advanced School on Exoplanetary Science, ed. K. Biazzo, V. Bozza, L. Mancini, & A. Sozzetti, 143–234
- Birkby, J. L., de Kok, R. J., Brogi, M., Schwarz, H., & Snellen, I. A. G. 2017, *AJ*, 153, 138
- Bonfils, X., Delfosse, X., Udry, S., et al. 2013, *A&A*, 549, A109
- Bonomo, A. S., Zeng, L., Damasso, M., et al. 2019, *Nature Astronomy*, 3, 416
- Borsa, F., Allart, R., Casasayas-Barris, N., et al. 2021a, *A&A*, 645, A24
- Borsa, F., Giacobbe, P., Bonomo, A. S., et al. 2022, *A&A*, 663, A141
- Borsa, F., Lanza, A. F., Raspantini, I., et al. 2021b, *A&A*, 653, A104
- Borsa, F., Rainer, M., Bonomo, A. S., et al. 2019, *A&A*, 631, A34
- Borucki, W. J., Koch, D., Basri, G., et al. 2010, *Science*, 327, 977
- Brogi, M., de Kok, R. J., Birkby, J. L., Schwarz, H., & Snellen, I. A. G. 2014, *A&A*, 565, A124
- Brogi, M., Giacobbe, P., Guilluy, G., et al. 2018, *A&A*, 615, A16
- Brogi, M., Line, M., Bean, J., Désert, J. M., & Schwarz, H. 2017, *ApJ*, 839, L2
- Brogi, M. & Line, M. R. 2019, *AJ*, 157, 114
- Brogi, M., Snellen, I. A. G., de Kok, R. J., et al. 2012, *Nature*, 486, 502
- Bryson, S., Kunimoto, M., Kopparapu, R. K., et al. 2021, *AJ*, 161, 36
- Cabot, S. H. C., Madhusudhan, N., Hawker, G. A., & Gandhi, S. 2019, *MNRAS*, 482, 4422
- Carleo, I., Giacobbe, P., Guilluy, G., et al. 2022, *AJ*, 164, 101
- Choksi, N. & Chiang, E. 2020, *MNRAS*, 495, 4192
- Ciardi, D. R., Fabrycky, D. C., Ford, E. B., et al. 2013, *ApJ*, 763, 41
- Cloutier, R., Charbonneau, D., Stassun, K. G., et al. 2021, *AJ*, 162, 79
- Cont, D., Yan, F., Reiners, A., et al. 2022, *A&A*, 668, A53
- Cosentino, R., Lovis, C., Pepe, F., et al. 2012, in *Society of Photo-Optical Instrumentation Engineers (SPIE) Conference Series*, Vol. 8446, *Ground-based and Airborne Instrumentation for Astronomy IV*, ed. I. S. McLean, S. K. Ramsay, & H. Takami, 84461V
- Damasso, M., Bonomo, A. S., Astudillo-Defru, N., et al. 2018, *A&A*, 615, A69
- Damasso, M., Perger, M., Almenara, J. M., et al. 2022, *A&A*, 666, A187
- Damasso, M., Sozzetti, A., Lovis, C., et al. 2020, *A&A*, 642, A31
- Deleuil, M., Aigrain, S., Moutou, C., et al. 2018, *A&A*, 619, A97
- Ehrenreich, D., Lovis, C., Allart, R., et al. 2020, *Nature*, 580, 597
- Endl, M., Cochran, W. D., Kürster, M., et al. 2006, *ApJ*, 649, 436
- Faria, J. P., Suárez Mascareño, A., Figueira, P., et al. 2022, *A&A*, 658, A115
- Fernandes, R. B., Mulders, G. D., Pascucci, I., Mordasini, C., & Emsenhuber, A. 2019, *ApJ*, 874, 81
- Fischer, D. A. & Valenti, J. 2005, *ApJ*, 622, 1102

- Fressin, F., Torres, G., Charbonneau, D., et al. 2013, *ApJ*, 766, 81
- Fulton, B. J. & Petigura, E. A. 2018, *AJ*, 156, 264
- Fulton, B. J., Petigura, E. A., Howard, A. W., et al. 2017, *AJ*, 154, 109
- Fulton, B. J., Rosenthal, L. J., Hirsch, L. A., et al. 2021, *ApJS*, 255, 14
- Ghezzi, L., Montet, B. T., & Johnson, J. A. 2018, *ApJ*, 860, 109
- Giacobbe, P., Brogi, M., Gandhi, S., et al. 2021, *Nature*, 592, 205
- Gillon, M., Triaud, A. H. M. J., Demory, B.-O., et al. 2017, *Nature*, 542, 456
- Guilluy, G., Andretta, V., Borsa, F., et al. 2020, *A&A*, 639, A49
- Guilluy, G., Giacobbe, P., Carleo, I., et al. 2022a, *A&A*, 665, A104
- Guilluy, G., Sozzetti, A., Brogi, M., et al. 2019, *A&A*, 625, A107
- Guilluy, G., Sozzetti, A., Giacobbe, P., Bonomo, A. S., & Micela, G. 2022b, *Experimental Astronomy*, 53, 655
- He, M. Y., Ford, E. B., & Ragozzine, D. 2019, *MNRAS*, 490, 4575
- He, M. Y., Ford, E. B., Ragozzine, D., & Carrera, D. 2020, *AJ*, 160, 276
- Holl, B., Sozzetti, A., Sahlmann, J., et al. 2022, *arXiv e-prints*, [arXiv:2206.05439](https://arxiv.org/abs/2206.05439)
- Howard, A. W. 2013, *Science*, 340, 572
- Howard, A. W., Marcy, G. W., Bryson, S. T., et al. 2012, *ApJS*, 201, 15
- Hsu, D. C., Ford, E. B., Ragozzine, D., & Ashby, K. 2019, *AJ*, 158, 109
- Johnson, J. A., Aller, K. M., Howard, A. W., & Crepp, J. R. 2010, *PASP*, 122, 905
- Kasper, M., Cerpa Urrea, N., Pathak, P., et al. 2021, *The Messenger*, 182, 38
- Kipping, D. M. 2013, *MNRAS*, 434, L51
- Kunimoto, M. & Matthews, J. M. 2020, *AJ*, 159, 248
- Lacedelli, G., Malavolta, L., Borsato, L., et al. 2021, *MNRAS*, 501, 4148
- Leleu, A., Alibert, Y., Hara, N. C., et al. 2021, *A&A*, 649, A26
- Luque, R. & Pallé, E. 2022, *Science*, 377, 1211
- Madhusudhan, N. 2019, *ARA&A*, 57, 617
- Madhusudhan, N., Knutson, H., Fortney, J. J., & Barman, T. 2014, in *Protostars and Planets VI*, ed. H. Beuther, R. S. Klessen, C. P. Dullemond, & T. Henning, 739
- Malavolta, L., Mayo, A. W., Louden, T., et al. 2018, *AJ*, 155, 107
- Maldonado, J., Micela, G., Baratella, M., et al. 2020, *A&A*, 644, A68
- Marconi, A., Abreu, M., Adibekyan, V., et al. 2021, *The Messenger*, 182, 27
- Mayor, M. & Queloz, D. 1995, *Nature*, 378, 355
- Mishra, L., Alibert, Y., Udry, S., & Mordasini, C. 2023, *arXiv e-prints*, [arXiv:2301.02374](https://arxiv.org/abs/2301.02374)
- Morbidelli, A., Bitsch, B., Crida, A., et al. 2016, *ICARUS*, 267, 368
- Mortier, A., Bonomo, A. S., Rajpaul, V. M., et al. 2018, *MNRAS*, 481, 1839
- Mortier, A., Santos, N. C., Sozzetti, A., et al. 2012, *A&A*, 543, A45
- Mulders, G. D., Ciesla, F. J., Min, M., & Pascucci, I. 2015, *ApJ*, 807, 9
- Nortmann, L., Pallé, E., Salz, M., et al. 2018, *Science*, 362, 1388
- Owen, J. E. & Wu, Y. 2017, *ApJ*, 847, 29
- Pepe, F., Cameron, A. C., Latham, D. W., et al. 2013, *Nature*, 503, 377
- Pepe, F., Cristiani, S., Rebolo, R., et al. 2021, *A&A*, 645, A96
- Petigura, E. A., Marcy, G. W., Winn, J. N., et al. 2018, *AJ*, 155, 89
- Pinamonti, M., Sozzetti, A., Maldonado, J., et al. 2022, *A&A*, 664, A65
- Pino, L., Désert, J.-M., Brogi, M., et al. 2020, *ApJ*, 894, L27
- Quanz, S. P., Absil, O., Benz, W., et al. 2021, *Experimental Astronomy* [[arXiv:1908.01316](https://arxiv.org/abs/1908.01316)]
- Rauer, H., Catala, C., Aerts, C., et al. 2014, *Experimental Astronomy*, 38, 249
- Sabotta, S., Schlecker, M., Chaturvedi, P., et al. 2021, *A&A*, 653, A114
- Salz, M., Czesla, S., Schneider, P. C., et al. 2018, *A&A*, 620, A97
- Schlaufman, K. C. 2014, *ApJ*, 790, 91
- Sebastian, D., Guenther, E. W., Deleuil, M., et al. 2022, *MNRAS*, 516, 636
- Snellen, I. A. G., de Kok, R. J., de Mooij, E. J. W., & Albrecht, S. 2010, *Nature*, 465, 1049
- Sousa, S. G., Adibekyan, V., Santos, N. C., et al. 2019, *MNRAS*, 485, 3981
- Sozzetti, A., Torres, G., Latham, D. W., et al.

- 2009, *ApJ*, 697, 544
- Struve, O. 1952, *The Observatory*, 72, 199
- Suárez Mascareño, A., Damasso, M., Lodieu, N., et al. 2021, *Nature Astronomy*, 6, 232
- Suárez Mascareño, A., Faria, J. P., Figueira, P., et al. 2020, *A&A*, 639, A77
- Taberner, H. M., Zapatero Osorio, M. R., Allart, R., et al. 2021, *A&A*, 646, A158
- Tinetti, G., Drossart, P., Eccleston, P., et al. 2018, *Experimental Astronomy*, 46, 135
- Tuomi, M., Jones, H. R. A., Barnes, J. R., Anglada-Escudé, G., & Jenkins, J. S. 2014, *MNRAS*, 441, 1545
- Turrini, D., Zinzi, A., & Belinchon, J. A. 2020, *A&A*, 636, A53
- Udry, S., Dumusque, X., Lovis, C., et al. 2019, *A&A*, 622, A37
- Wang, M.-T., Liu, H.-G., Zhu, J., & Zhou, J.-L. 2021, *AJ*, 162, 258
- Weiss, L. M., Marcy, G. W., Petigura, E. A., et al. 2018, *AJ*, 155, 48
- Wittenmyer, R. A., Wang, S., Horner, J., et al. 2020, *MNRAS*, 492, 377
- Wolthoff, V., Reffert, S., Quirrenbach, A., et al. 2022, *A&A*, 661, A63
- Wright, J. T., Upadhyay, S., Marcy, G. W., et al. 2009, *ApJ*, 693, 1084
- Yang, J.-Y., Xie, J.-W., & Zhou, J.-L. 2020, *AJ*, 159, 164
- Zeng, L., Jacobsen, S. B., Sasselov, D. D., et al. 2019, *Proceedings of the National Academy of Science*, 116, 9723